Enantioselective Construction of the Cycl[3.2.2]azine Core via Organocatalytic [12 + 2] Cycloadditions

Enantioselective Construction of the Cycl[3.2.2]azine Core *via* Organocatalytic [12+2] Cycloadditions

Nicolaj Inunnguaq Jessen, Giulio Bertuzzi, Maksimilian Bura, Mette Louise Skipper and Karl Anker Jørgensen*

Department of Chemistry, Aarhus University, DK-8000 Aarhus C, Denmark

ABSTRACT

The first enantioselective [12+2] cycloaddition for the construction of a chiral cycl[3.2.2]azine core—a tricyclic moiety with a central ring-junction nitrogen atom—by an operationally simple one-step organocatalytic process, has been developed. The reaction concept builds upon aminocatalytically generated 12π-components derived from 5*H*-benzo[*a*]pyrrolizine-3-carbaldehydes reacting with different electron-deficient 2π-components and affording the complex scaffold of benzo[*a*]cycl[3.2.2]azine (indolizino[3,4,5-*ab*]isoindole) with excellent enantio- and diastereoselectivity in good yields. The developed reaction is robust toward diverse substituent patterns and has been extended to different classes of electron-deficient 2π-components by minor variations in reaction setup. The obtained [12+2] cycloadducts are electron-deficient in nature and their reaction with nucleophiles have been demonstrated. The enantioselective [12+2] cycloaddition for α,β-unsaturated aldehydes as the electron-deficient 2π-components relies upon an unconventional, simple aminocatalyst. In order to understand the high stereoselectivity of the [12+2] cycloaddition for this simple catalyst, combined experimental and computational investigations were performed. The investigations point to activation of both the 5*H*-benzo[*a*]pyrrolizine-3-carbaldehyde and the α,β-unsaturated aldehyde by the aminocatalyst and that the reaction proceeds by a stepwise cycloaddition, where both the initial conjugate addition, as well as ring-closure are crucial for the stereochemical outcome. For other electron-deficient 2π-components, such as α,β-unsaturated ketoesters and nitroolefins, a more sterically demanding aminocatalyst has been applied and the corresponding [12+2] cycloadducts are obtained with excellent stereoselectivity. The [12+2] cycloaddition with vinyl sulfones afforded fully unsaturated systems, which display photoluminescence properties and for which quantum yields have been evaluated.

INTRODUCTION

The construction of structurally complex molecular scaffolds traditionally relies on long synthetic sequences to ensure selective transformations. In recent years, organocatalytic higher-order cycloadditions have emerged as an efficient tool for the controlled formation of complex cyclic systems in a single synthetic step.[1] Through aminocatalytic generation, inherently unstable π-components of extended conjugation can be wielded under ambient conditions, and their utilization in cycloaddition chemistry can provide products which are unobtainable through traditional Diels-Alder processes. The development of such unorthodox cycloaddends expands the range of compounds accessible through cycloaddition chemistry.

Cyclic structures containing ring-junction nitrogen atoms are abundant in naturally occurring alkaloids.[2] Cyclazines, named so by Boekelheide in 1959,[3] consist of a tricyclic core with a central nitrogen atom. Specifically, the cycl[3.2.2]azine core (pyrrolo[2,1,5-*cd*]indolizine, Figure 1) has been found in the natural product vlasoulamine A,[4] as well as in a variety of saturated compounds belonging to the family of myrmicarins (see *e.g.* myrmicarin 215A**Errore. L'origine riferimento non è stata trovata.**).[5] Several unsaturated cycl[3.2.2]azine derivatives, such as NNC 45-0095, have displayed high activity as non-steroidal agonists for the estrogen receptor through mimicking the steroid core with their tricyclic nucleus.[6] In addition to these biological prospects, related benzo[*a*]cycl[3.2.2]azines (indolizino[3,4,5-*ab*]isoindoles) have drawn interest as potent organic fluorophores.[7]

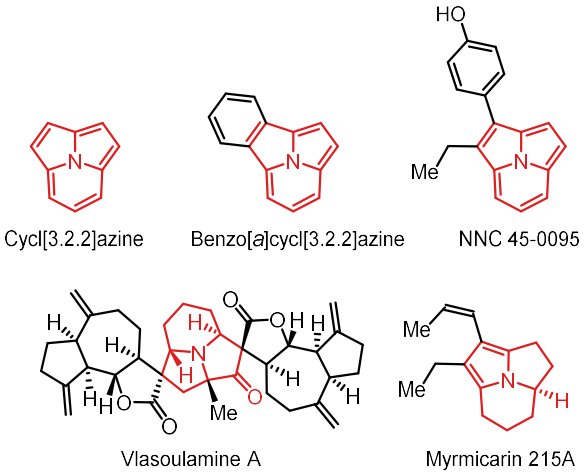

Figure 1: Tricyclic alkaloids containing a ring-junction nitrogen atom.

The cycl[3.2.2]azine core has historically been accessed through annulation of substituted indolizines, as illustrated by Boekelheide,[3] or of 3*H*-pyrrolizine with vinamidinium salts.[8] Other elegant strategies rely on cycloaddition chemistry, such as double 1,3-dipolar cycloadditions of pyridinium salts (Figure 2a),[9] or cycloadditions of indolizines and dialkyl acetylenedicarboxylates.[10,11] While the latter reaction type depends on dehydrogenation or elimination to give stable, fully unsaturated cyclazines, one report shows the racemic formation of oxidatively labile benzo[*a*]cycl[3.2.2]azines (Figure 2b).[12] Alternatively, the usage of 3-methylenic 3*H*-pyrrolizine derivatives in [8+2] cycloadditions enables the construction of the 6-membered ring of cycl[3.2.2]azines.[13] Despite the elegance of these sporadic reactions, examples of non-racemic procedures are limited to multistep chiral pool syntheses of the myrmicarins.[14] While convenient pathways toward fully unsaturated or racemic cycl[3.2.2]azines have been exemplified, *stereocontrolled counterparts suffer from poor accessibility*. The challenge for the enantioselective construction of such a structurally complex alkaloid core in a simple manner encouraged us to pursue the synthesis of chiral benzo[*a*]cycl[3.2.2]azines, harnessing the strengths of aminocatalytic higher-order cycloadditions.

Here, we present the first enantioselective pathway toward chiral benzo[*a*]cycl[3.2.2]azines proceeding in a single reaction step, based on a catalytic formal [12+2] cycloaddition (Figure 2c). The activation of benzo[*a*]pyrrolizine-3-carbaldehydes facilitates reactivity toward a diverse pool of 2π-components by an organocatalytic process under simple reaction conditions. Catalytic examples of cognate 14π-electron processes—[10+4] cycloadditions—were previously described,[15] but, to the best of our knowledge, only sparse non-catalytic [12+2] cycloadditions precede this report.[12,16]

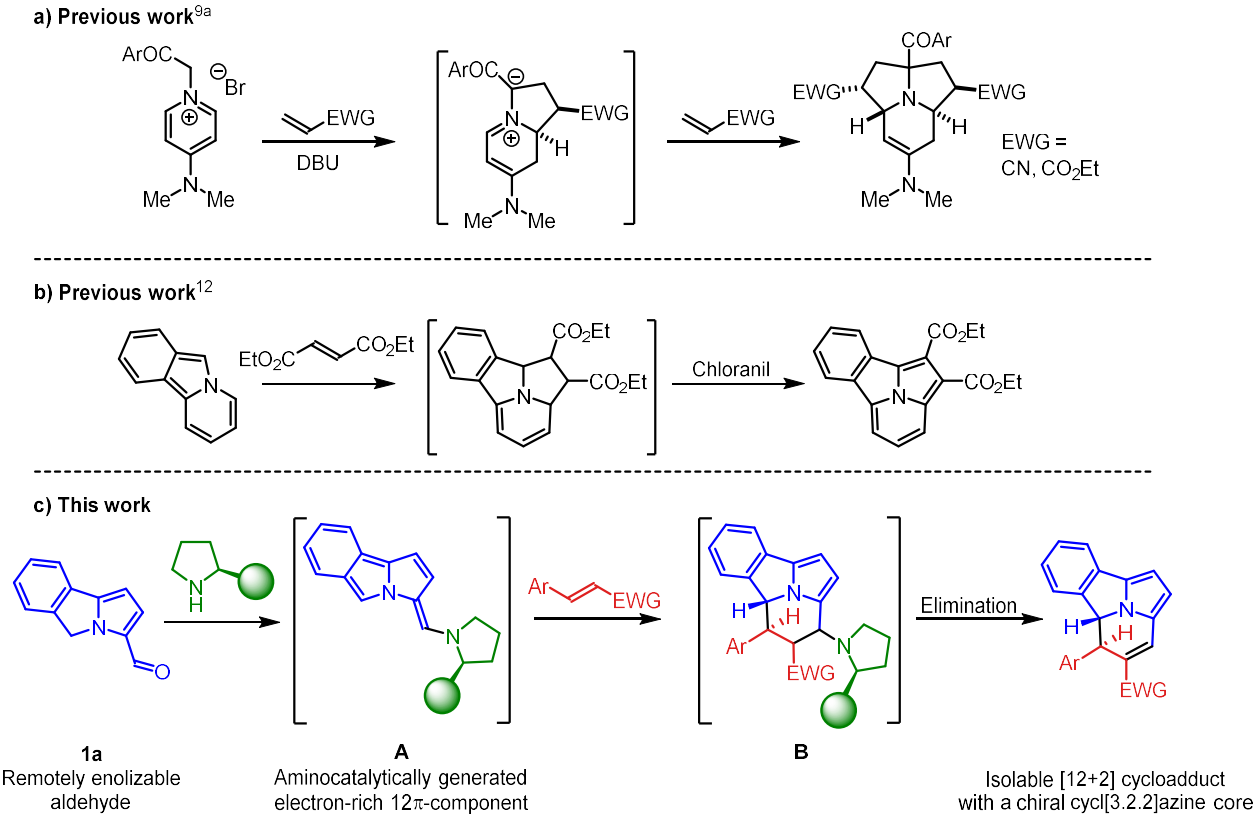

Figure 2: Construction of the cycl[3.2.2]azine core through cycloaddition chemistry.

RESULTS AND DISCUSSION

Reaction design. Vinylogous aminocatalysis allows for the generation of reactive polyenes by deprotonation of enolizable aldehydes in remote positions.[17] The utilization of this strategy was envisioned to furnish an electron-rich 12π-component intermediate **A** from 5*H*-benzo[*a*]pyrrolizine-3-carbaldehyde **1a** (Figure 2c). By condensation of the aldehyde handle with an aminocatalyst, an extended π-system is revealed which reacts initially as a nucleophile and subsequently as an electrophile through the exocyclic position. This enables higher-order cycloadditions with electron-poor 2π-components to construct the 6-membered ring of a cycl[3.2.2]azine core, followed by eliminative release of the aminocatalyst from intermediate **B**. It is notable that the elimination step also removes the aldehyde handle, forming an olefin and thereby allowing for further stereoselective diversification of the chiral core. Even-membered ring syntheses based on higher-order cycloadditions are rare, but become possible in this case due to the usage of a cycloaddend containing a ring-junction nitrogen atom.

Initially, the reaction of 5*H*-benzo[*a*]pyrrolizine-3-carbaldehyde **1a** with 4-bromocinnamaldehyde **2a** (1.5 equiv.), catalyzed by pyrrolidine and benzoic acid (both 20 mol%) in $CDCl_3$, was found to provide the [12+2] cycloadduct **3a** in 51% NMR yield with a diastereoselectivity of 2.6:1 in favor of the *trans*-adduct (Table 1, entry 1). In addition to the cycloadduct **3a**, a Michael adduct **C** of **1a** and **2a** was observed in low amounts, indicating the existence of a stepwise, formal cycloaddition pathway. The application of diphenylprolinol silyl ether catalyst **I** furnished **3a** with exceptional enantioselectivity and increased

diastereoselectivity, showing the potential to form the chiral core with a great degree of stereocontrol (entry 2). However, only low conversion was attained and efforts to increase the yield using **I** were unsuccessful. Due to the probable activation of both π-components, and thus the involvement of two catalyst molecules in the stereodetermining step, the very simple catalyst **II** was examined and delivered **3a** with 55% ee, maintaining the diastereoselectivity (entry 3). To support the operation of a dual catalytic system, a positive non-linear effect has been established (*vide infra*). Gradual increments of the catalysts' steric demand (entries 4, 5) revealed the unconventional prolinol silyl ether **IV**[18] as a promising candidate. Other silyl ether groups (OTIPS, OTBS, OTPS; see Supporting Information) were found to induce lower degrees of stereoselectivity. Decreasing the solvent volume had no adverse effects (entry 6), and conducting the reaction at 30 °C improved both the enantio- and diastereoselectivity of the reaction slightly. The presence of an acid additive proved necessary for the reaction to proceed, and among various benzoic acid derivatives, the use *o*-FBzOH was found to induce a slight increase in enantioselectivity. A screening of solvents did not improve the yield and stereoselectivity of the cycloaddition, although chlorinated solvents ($CDCl_3$, CH_2Cl_2, 1,2-DCE, PhCl) were found to facilitate the reaction, while the use of other solvents (THF, MeCN, PhMe) led to vastly inferior conversion rates. The developed method is capable of producing the [12+2] cycloadduct **3a** with high selectivity toward the *trans*-adduct (55% NMR yield, 17:1 crude d.r. 91% ee). However, the major *trans*-diastereoisomer converts partially and irreversibly into the minor *cis*-diastereoisomer during purification *via* flash chromatography, dependent on residence time, leading to an erosion in diastereomeric ratio in spite of differing R_f values for these isomers. While the minor diastereoisomer *cis*-**3a** which formed in the reaction vessel (entry 8) showed 40% ee, the quantity of *cis*-**3a** found in the major diastereoisomer *trans*-**3a** fraction was determined to be racemic. This witnesses the existence of a separate pathway involving an unobserved achiral intermediate which is responsible for the irreversible interconversion of diastereoisomers (*vide infra*). The isolated Michael adduct **C** (using reaction conditions of Table 1, entry 8) was likewise obtained in 40% ee, and only *cis*-**3a** was formed upon re-subjection to the optimized reaction conditions, with very low conversion. The formation of **C** is therefore irreversible and originates from a pathway toward *cis*-**3a**.

Table 1: Optimization of the [12+2] cycloaddition of 5*H*-benzo[*a*]pyrrolizine-3-carbaldehyde **1a** with 4-*trans*-bromocinnamaldehyde **2a** for the formation of cycloadduct **3a**.

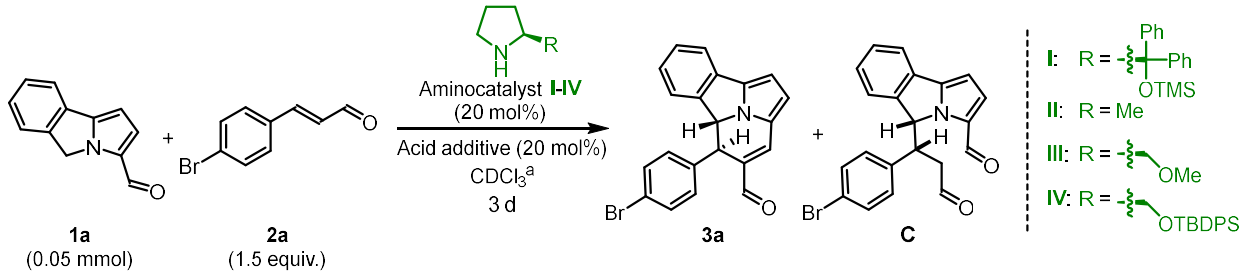

Entry	Catalyst	Additive	Solvent V (mL)	Temp. (°C)	NMR yield of **3a** (%)[b]	d.r. of **3a** (crude)	ee of **3a**[c] (%)	NMR yield of **C** (%)
1	Pyrrolidine	BzOH	0.3	40	51	2.6:1	-	5
2	**I**	BzOH	0.3	40	17	7.5:1	99	5
3	**II**	BzOH	0.3	40	34	7.5:1	55	10
4	**III**	BzOH	0.3	40	45	6.5:1	65	11
5	**IV**	BzOH	0.3	40	54	12:1	89	12
6	**IV**	BzOH	0.1	40	55	13:1	88	10
7	**IV**	BzOH	0.1	30	54	17:1	90	11
8	**IV**	*o*-FBzOH	0.1	30	55 (52[d])	17:1 (6:1[d])	91	13

[a] Filtered through basic alumina prior to reaction setup. [b] Combined NMR yields of both diastereoisomers of **3a**. [c] Value of isolated **3a** determined by UPC[2]. [d] Values of isolated product.

Reaction scope – part I. The effects of varying the substrate substituent patterns in the developed strategy toward enantioenriched benzo[*a*]cycl[3.2.2]azines were examined as shown in Figure 3. Due to the stereochemical lability of the major diastereoisomers of cycloadducts **3a**–**r** during purification, these cycloadducts were subjected to a robust one-pot reduction of the aldehyde group in parallel experiments. This transformation yielded the corresponding allylic alcohols (**3a'**–**r'**) which are stereochemically stable and isolable with preservation of the high diastereoselectivity of the formal [12+2] cycloaddition. The developed process delivers the envisioned cycloadducts with highly consistent enantioselectivities for a range of substituent patterns. Compared to the standard reaction toward **3a**/**3a'**, the use of cinnamaldehyde or electron-rich variations provided cycloadducts **3b**/**3b'**, **3d**/**d'**, **3e**, **3f'**, **3g'** in increased yields. Both *o*-, *m*-, and *p*-substituents are therefore tolerated, although the *o*-substituted adduct **3e** was obtained with a lower diastereoselectivity. The electron-poor *p*-trifluoromethyl-substituted adduct **3c** was formed with slightly lower selectivity and yield. Alcohols **3c'** and **3e'** displayed an increased lability during purification, preventing their isolation. Potential utilization of heterocyclic 2π-components was demonstrated by the isolation of adducts **3h**/**3h'**.

Various substituted 5*H*-benzo[*a*]pyrrolizine-3-carbaldehydes **1**, available through two-step procedures from commercially available starting materials,[19] were likewise found to behave consistently in the developed reaction. Products carrying electron-withdrawing substituents in the 8-position (**3i'**, **3j**/**3j'**) were formed with higher stereoselectivity, but lower yields than 8-methoxysubstituted product **3l**; 8-bromosubstituted **3k'** was formed with both high selectivity and yield. The 8-*tert*-butyl adduct **3m'** was formed in 45% yield and the 7,9-dimethylsubstituted adducts **3q**/**3q'** were obtained under harsher conditions. The 7-trifluoromethylsubstituted products **3p**/**3p'** were obtained with good results. As expected, the presence of substituents in the 6-position (adjacent to the reactive site of **1**) impeded the cycloaddition and entailed a lowered reactivity as well as stereoselectivity toward the adducts **3n** and **3o**. The adduct **3o** was especially labile toward diastereomer interconversion and the *cis*-diastereoisomer was obtained as the major product. The efficient formation of adducts **3r**/**3r'** demonstrated the potential of substituting the pyrrole moiety of the cycl[3.2.2]azine core. Despite attempts, non-benzofused 3*H*-pyrrolizine-5-carbaldehyde has not been brought to participate in the developed cycloaddition reaction. This indicates that the 4π-electrons of the benzofused ring in **1** are involved in the reactions and therefore this fragment is not acting as a spectator during the cycloaddition.

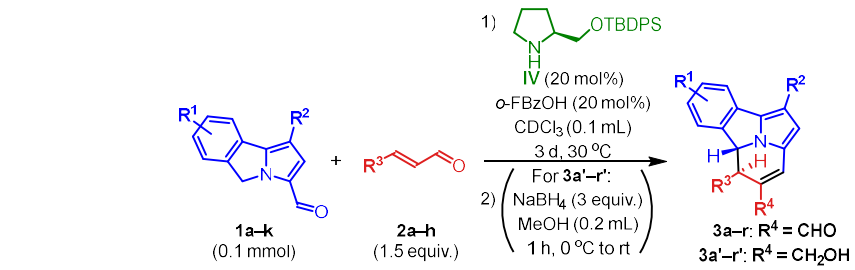

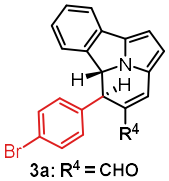

3a: R⁴ = CHO
52% yield, 91% ee
d.r. 2.9:1 (>20:1)
3a': R⁴ = CH₂OH
49% yield, 91% ee
d.r. >20:1

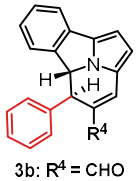

3b: R⁴ = CHO
62% yield, 90% ee
d.r. 3.8:1 (>20:1)
3b': R⁴ = CH₂OH
60% yield, 89% ee
d.r. >20:1

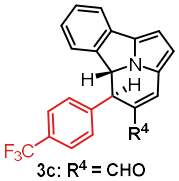

3c: R⁴ = CHO
47% yield, 88% ee
d.r. 4.3:1 (14:1)
3c': R⁴ = CH₂OH
n.d.[a]

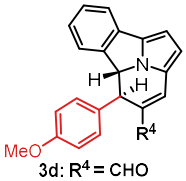

3d: R⁴ = CHO
84% yield, 92% ee
d.r. 3.0:1 (>20:1)
3d': R⁴ = CH₂OH
61% yield, 91% ee
d.r. >20:1

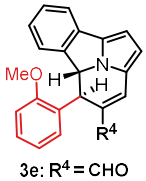

3e: R⁴ = CHO
64% yield, 89% ee
d.r. 4.0:1 (10:1)
3e': R⁴ = CH₂OH
n.d.[a]

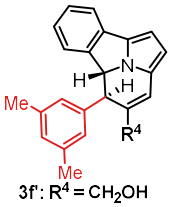

3f': R⁴ = CH₂OH
59% yield, 91% ee
d.r. >20:1

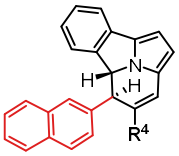

3g': R⁴ = CH₂OH
58% yield, 89% ee
d.r. >20:1

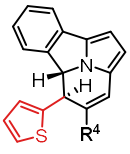

3h: R⁴ = CHO
35% yield, 90% ee
d.r. 4.5:1 (7:1)
3h': R⁴ = CH₂OH
39% yield, 92% ee
d.r. >20:1

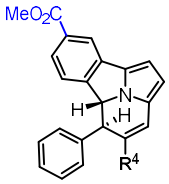

3i': R⁴ = CH₂OH
39% yield, 90% ee
d.r. >20:1

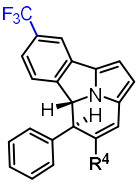

3j: R⁴ = CHO
48% yield, 91% ee
d.r. 11:1 (>20:1)
3j': R⁴ = CH₂OH
48% yield, 90% ee
d.r. >20:1

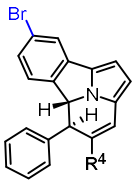

3k': R⁴ = CH₂OH
61% yield, 92% ee
d.r. >20:1

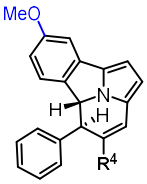

3l: R⁴ = CHO
56% yield, 89% ee
d.r. 2.4:1 (16:1)
3l': R⁴ = CH₂OH
n.d.[a]

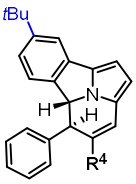

3m': R⁴ = CH₂OH
45% yield, 91% ee
d.r. >20:1

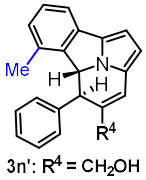

3n': R⁴ = CH₂OH
22% yield, 73% ee
d.r. 2.1:1

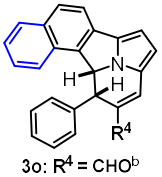

3o: R⁴ = CHO[b]
23% yield, 5% ee
d.r. >20:1 (5:1)
3o': R⁴ = CH₂OH
n.d.[c]

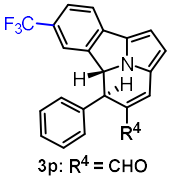

3p: R⁴ = CHO
65% yield, 93% ee
d.r. 1.3:1 (>20:1)
3p': R⁴ = CH₂OH
56% yield, 91% ee
d.r. >20:1

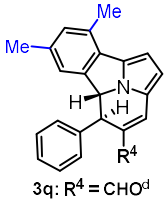

3q: R⁴ = CHO[d]
56% yield, 89% ee
d.r. 1.6:1 (8:1)
3q': R⁴ = CH₂OH[d]
58% yield, 90% ee
d.r. >20:1

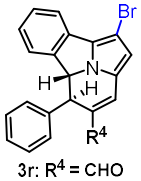

3r: R⁴ = CHO
67% yield, 92% ee
d.r. 3.4:1 (12:1)
3r': R⁴ = CH₂OH
69% yield, 92% ee
d.r. >20:1

Isolated yields. The solvent was filtered through basic alumina prior to reaction setup. Diastereomeric ratios determined by NMR analysis of isolated product; ratios obtained from crude reaction mixtures are given in parentheses. The enantiomeric excess values were determined by UPC[2]. [a] Decomposition during chromatographic purification. [b] Product isolated as the *cis*-diastereoisomer. [c] Reduction of the aldehyde did not proceed. [d] Reaction run for 4 d at 40 °C.

Figure 3: Scope for the [12+2] cycloaddition of 5*H*-benzo[*a*]pyrrolizine-3-carbaldehydes **1** with α,β-unsaturated aldehydes **2** for the formation of cycloadducts **3**.

The absolute configuration of cycloadduct **3h'** was determined by comparison between calculated and experimental electronic circular dichroism (ECD) spectra (see Supporting Information). The experimentally obtained ECD spectrum is in good agreement with the spectrum obtained using time-dependent density functional theory (TD-DFT) for *trans*-(*R*,*R*)-**3h'**. Due to the high level of consistency in stereoselectivity, the remaining cycloadducts **3** have been assigned by analogy. The reliability of ECD for assignment of the absolute configuration of the [12+2] cycloadducts was further corroborated by X-ray analysis (*vide infra*).

Mechanistic investigations. The present aminocatalytic cycloaddition toward benzo[*a*]cycl[3.2.2]azines presented in Part I utilize two conjugated aldehydes, and the operation of a dual catalytic system was established through the observation of a positive non-linear effect through the application of catalyst **IV** exhibiting various degrees of enantiomeric excess (Figure 4a).[20] The existence of a mismatch in the activity of enantiomeric catalysts was substantiated by the observation that conversion of starting material into product is slower when using less enantioenriched catalyst (Figure 4b). Increased amounts of Michael adduct **C** were present when using catalyst with lower enantiomeric excess, indicating that a catalyst mismatch increases the energetic barrier of ring-closure.

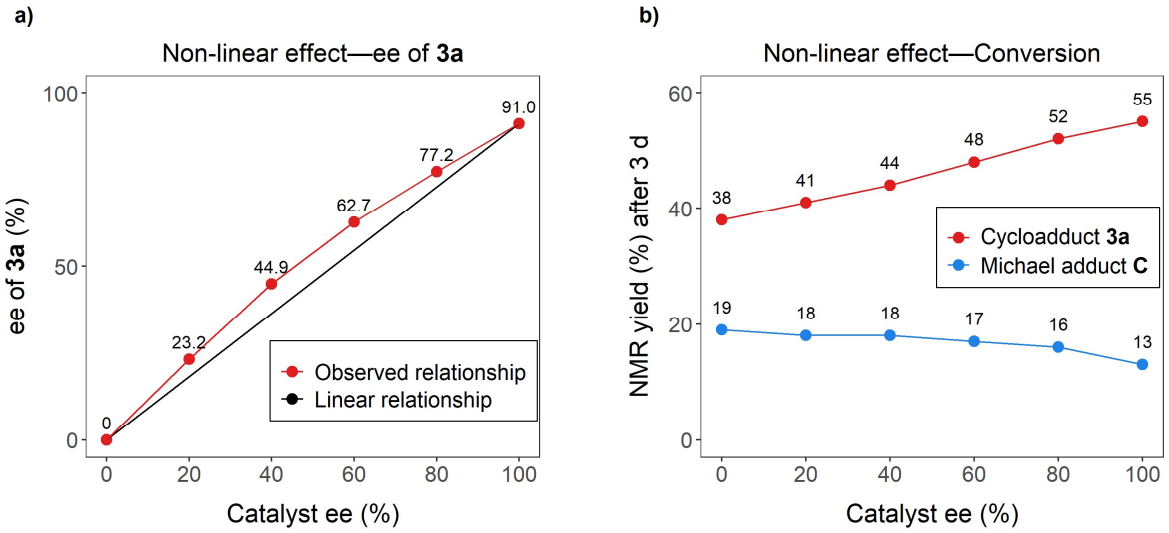

Figure 4: Non-linear effects on the [12+2] cycloadduct **3a** derived from varying the enantiomeric excess of aminocatalyst **IV**. Reaction conditions were otherwise identical to those given in Table 1, entry 8.

In order to rationalize the high level of stereoselectivity of the [12+2] cycloaddition, the reaction steps central to the stereochemical outcome of the reaction have been studied computationally. Transition state (TS) structures for conjugate additions and ring-closures with aminocatalyst **IV** toward *trans*-(*R*,*R*)-**3b**, *trans*-(*S*,*S*)-**3b**, *cis*-(*R*,*S*)-**3b** and *cis*-(*S*,*R*)-**3b** were generated through systematic conformational searches with *Gaussian09*[21] using DFT [B3LYP/6-31G*].[22] Based on the resulting geometries, single point energy calculations were performed using [B3LYP-GD3(BJ)/def2TZVPP/SMD($CHCl_3$)].[23] Ground state structures were generated through re-optimized geometries obtained from intrinsic reaction coordinate (IRC) calculations of both lowest-energy TSs for each of the four stereoisomeric pathways toward **3b**. The computed free energy barriers were obtained by adding the free energy correction from the B3LYP/6-31G*

optimization to the single point calculations, and are given relative to the summed energies of iminium-ion **Int-1**, **1a** and **IV** (Figure 5). Stereoisomeric ratios were evaluated at 30 °C. For details on the conformational analyses and results using different levels of theory, see the Supporting Information.

The computational investigations in Figure 5a start with the iminium-ion **Int-1** derived from condensation of cinnamaldehyde **2b** with catalyst **IV**, along with 5*H*-benzo[*a*]pyrrolizine-3-carbaldehyde **1a**, and a second molecule of **IV**. These constitute the reference point (0.00 kcal/mol). Condensation of **1a** with **IV** generates the reactive 12π-component. Complexation between the two π-components generates four reactive complexes, of which the one initiating the *trans*-(*R*,*R*)-pathway (marked in blue) is lowest in energy. Through the first transition state **TS-1**, the first C—C-bond is formed, providing conjugate adducts which have to rotate around the newly generated bond in order to undergo the ring-closure step through **TS-2**, affording the cyclized intermediates. Upon elimination and hydrolysis of two molecules of catalyst **IV**, the observed [12+2] cycloadduct **3b** is formed.

Our findings suggest that the pathways for the four stereoisomers of **3b** involve TSs toward ring-closure which are higher in energy than for the initial conjugate addition. For each stereoisomeric pathway, the TS structures which were found to be lowest in energy are illustrated in Figure 5b; graphics of the actual geometries are enclosed in the Supporting Information.

The experimentally established major product *trans*-(*R*,*R*)-**3b** is calculated to be favored, although these results do not exclude the possibility that the catalyst release mechanisms or prerequisite condensation reactions influence the stereochemical outcome. The isolability of Michael adduct **C** (Table 1) could indicate that premature hydrolysis of aminocatalysts prior to cyclization is hardly reversible. Importantly, no TS for a concerted cycloaddition has been found computationally.

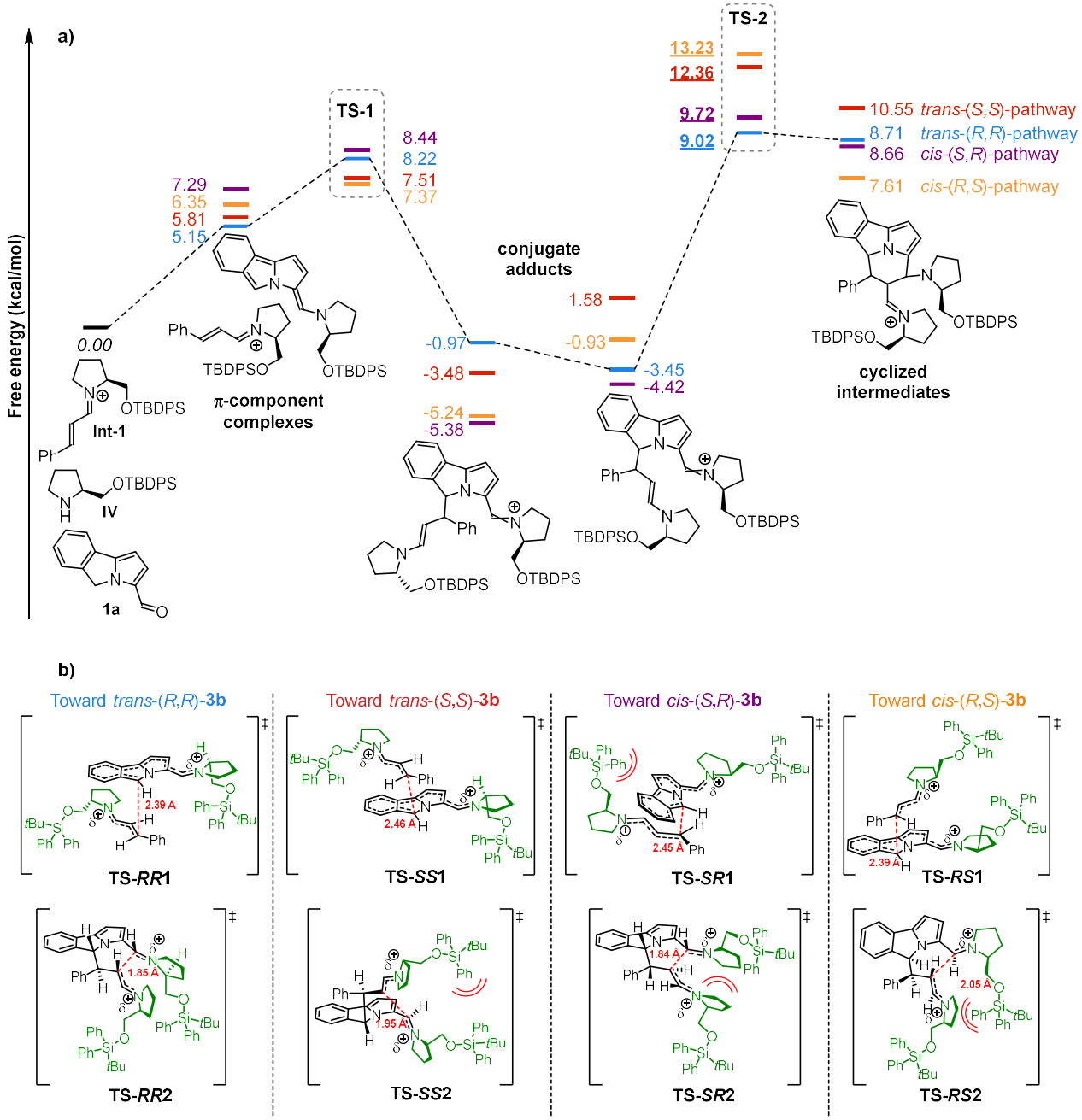

Figure 5: **a**) Lowest-energy pathways for the stereoisomers of **3b** calculated using DFT on the B3LYP-GD3(BJ)/def2TZVPP/SMD($CHCl_3$) level of theory. **b**) TS structures of lowest energy pathways depicted in **a**.

On the enantioselectivity. A lower activation energy was found for the conjugate addition toward *trans*-(*S*,*S*)-**3b** than for *trans*-(*R*,*R*)-**3b** (through **TS-*RR*1** or **TS-*SS*1**, respectively; see Figure 5b). Both proceed from the 12π-component derived from **1a** containing an s-*cis* enamine functionality, which, due to the flexibility of catalyst **IV**, is not significantly shielded on either face of the benzopyrrolizine moiety. As *trans*-(*R*,*R*)-**3b** is formed experimentally as the major product, the energetic relationship of **TS-*RR*1** and **TS-*SS*1** does not account for the observed enantioselectivity, indicating that the initial conjugate addition is reversible and under Curtin-Hammett control. Ring-closure toward *trans*-(*S*,*S*)-**3b** (through **TS-*SS*2**) is

disfavored due to the sterics of the aminocatalysts, giving rise to a calculated $\Delta\Delta G^{\ddagger}$ value for these enantiomeric pathways of 3.34 kcal/mol, corresponding to 99% ee in favor of *trans*-(*R*,*R*)-**3b**, in agreement with the experimentally established 90% ee.

On the diastereoselectivity. The initial conjugate addition toward *cis*-(*S*,*R*)-**3b** was calculated to proceed through **TS-*SR*1**, where a nucleophilic attack occurs on the face of the iminium-ion of cinnamaldehyde which is also occupied by the bulky group of the catalyst; however, due to the flexibility of the catalyst **IV**, this face is not significantly shielded. Ring-closure through **TS-*SR*2** is calculated to be disfavored due to a steric clash of the pyrrolidine moieties of the two catalysts. This interaction imposes a $\Delta\Delta G^{\ddagger}$ value of the *trans*-(*R*,*R*) and *cis*-(*S*,*R*) diastereomeric pathways of 0.70 kcal/mol, corresponding to a diastereomeric ratio of 3.2:1, a value which is smaller than what has been experimentally observed (>20:1 d.r. in the crude reaction mixture of **3b**, as well as for isolated product **3b'**). The most endergonic reaction step found was the ring-closure through **TS-*RS*1** which is impeded by a clash of the two catalyst units, rendering the formation of *cis*-(*R*,*S*)-**3b** disfavored. In contrast to **TS-*RR*1** and **TS-*SS*1**, both **TS-*SR*1** and **TS-*RS*1** proceed through enamine s-*trans* conformers of the 12π-component, opening the possibility of further stereodiscrimination during the initial condensation reaction.

The computational studies are thus in agreement with the experimental finding that the *trans*-(*R*,*R*) adducts **3** are formed as the major stereoisomers by a stepwise mechanism and indicate that especially the ring-closure TSs are of fundamental importance for the stereochemical outcome of the [12+2] cycloaddition.

A proposed mechanism for the observed interconversion from enantioenriched adducts *trans*-(*R,R*)-**3** to racemic *cis*-**3** adducts during purification on silica gel is illustrated in Figure 6. Activation of the α,β-unsaturated aldehyde functionality could facilitate bond cleavage through Grob-like fragmentation to give an achiral intermediate. The favored formation of an (*E*)-configured achiral intermediate would cause a subsequent ring-closure to produce *cis*-**3** which, due to free rotation of the intermediate, is formed as a racemate. On the contrary, a (*Z*)-configured achiral intermediate would lead to the formation of racemic *trans*-**3**. As for this isomer, no erosion is observed for the enantiomeric excess, fragmentation to such (*Z*)-configured achiral intermediate does not occur.

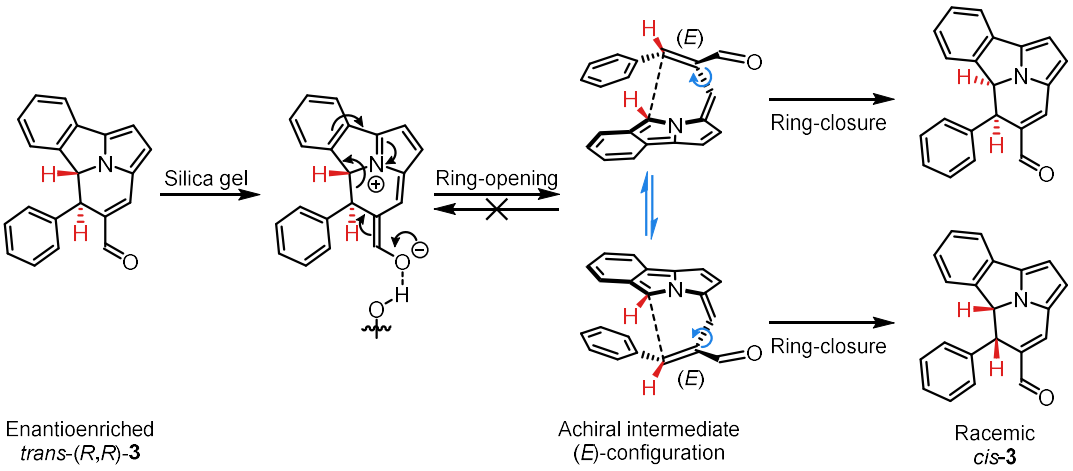

Figure 6: Proposed mechanism for the irreversible diastereomeric interconversion of cycloadducts **3** during chromatographic purification on silica gel.

Reaction scope – part II. While the aldehyde functional group is readily convertible to a range of other common substituents, we desired to expand the scope of the [12+2] cycloaddition to include the use of

diverse electron-deficient 2π-components. The application of such substrates renders the strategy of dual aminocatalytic activation unfeasible, meaning that higher temperatures are required for cycloadduct formation. Furthermore, the induced stereoselectivity depends on only one catalyst molecule, increasing the demand on its stereodirecting capabilities. Despite these challenges, α,β-unsaturated ketoesters **4a**–**d**, nitroolefins **4e**–**g** and an α,β-unsaturated trifluoromethyl ketone **4h** participate in the formation of [12+2] cycloadducts **5a**–**h** with minor variations in reaction setup (Figure 7). Individual optimization tables are given in the Supporting Information.

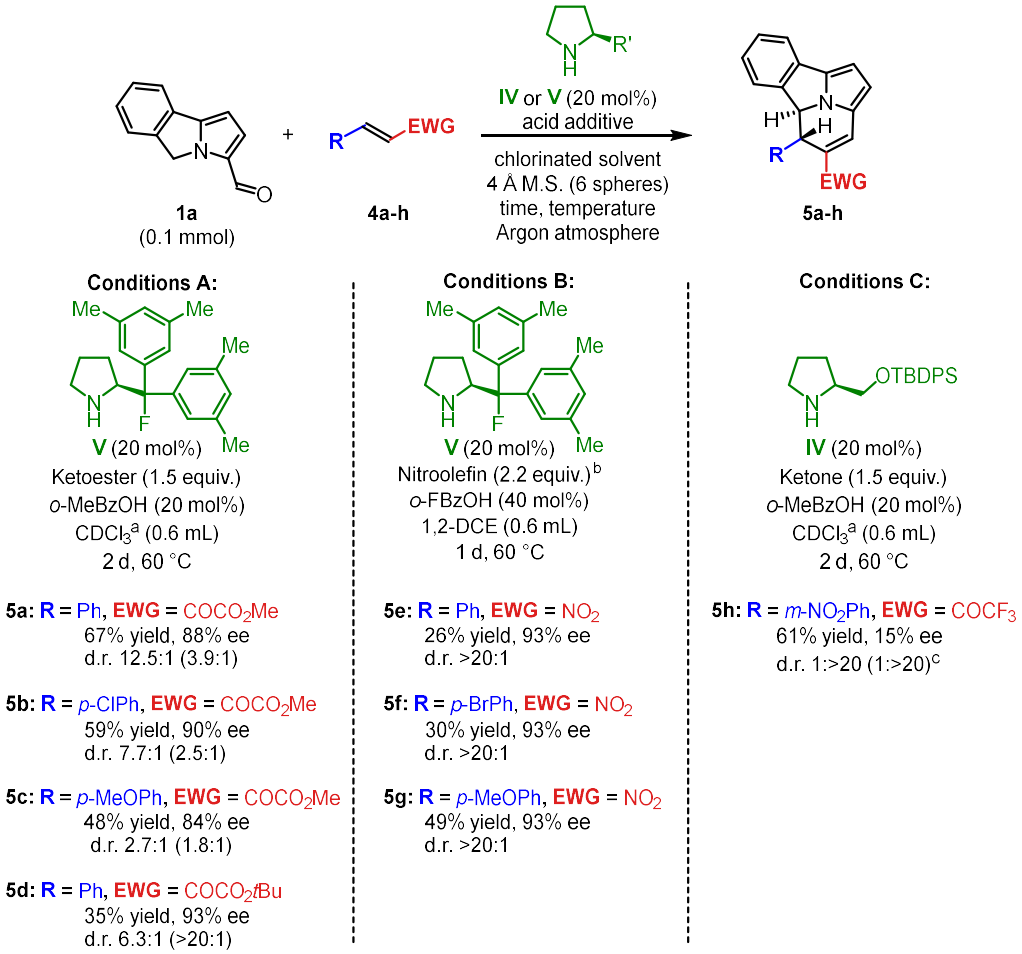

Isolated yields. Diastereomeric ratios determined by NMR analysis of isolated product; ratios obtained from crude reaction mixtures are given in parentheses. The enantiomeric excess values were determined by UPC[2]. [a] Filtered through basic alumina prior to reaction setup. [b] 1.2 Equivalents of nitroolefin added initially; one additional equivalent added after 8 h. [c] Product isolated as the *cis*-diastereoisomer.

Figure 7: Scope for the [12+2] cycloaddition of benzo[*a*]pyrrolizine-3-carbaldehyde **1a** with α,β-unsaturated ketoesters **4a**–**d**, nitroolefins **4e**–**g** and an α,β-unsaturated trifluoromethyl ketone **4h** for the formation of cycloadducts **5**.

In the pathway toward the cycloadducts derived from 2π-components **4**, the post-cyclization intermediate does not require hydrolysis to give the final product, and it was found that removal of water through the presence of molecular sieves could assist in driving the reaction forward. Using aminocatalyst **V** at 60 °C in either 1,2-dichloroethane (1,2-DCE) or $CDCl_3$ and with a benzoic acid additive, cycloadducts **5a**–**g** were obtained in 26-67% yield with high enantioselectivities (84-93% ee). Although the ketoester products **5a**–

d were formed with moderate diastereoselectivities, chromatographic separation typically improved the diastereomeric ratio of isolated material. Nitro-substituted adducts **5e**–**g** were formed and isolated with >20:1 d.r. These are, however, prone to partial aerobic oxidation under the reaction conditions to give fully unsaturated benzo[*a*]cycl[3.2.2]azines, necessitating their preparation to be conducted under an inert atmosphere. Importantly, a comparison of ECD spectra calculated using TD-DFT with experimentally obtained values indicated that the cycloadduct **5g** was formed with similar but *inverted* enantioselectivity compared to products **3**, delivering *trans*-(*R*,*S*)-**5g** as the major stereoisomer. This observation was corroborated through X-ray crystallographic analysis of **9** (obtained through a transformation of cycloadduct **5g**, *vide infra*). The stereochemistry of cycloadducts **5a**–**f**, likewise formed with catalyst **V**, was assigned by analogy. The absolute configuration of trifluoromethyl ketone-substituted **5h** has not been determined due to low enantiomeric excess; this compound could, however, be isolated in good yield and high diastereoselectivity toward the *cis*-adduct.

A rationale for the diverging enantioselectivities toward cycloadducts **3** and **5** may lie in the differences of the employed aminocatalysts (Figure 8). The reactive s-*cis* enamine moiety of **1a** and catalyst **IV** is not significantly shielded on either the *Re*- or *Si*-faces due to the flexibility of catalyst **IV**; the high stereoselectivity of reactions toward **3** is highly dependent on the second catalyst unit condensed with the α,β-unsaturated aldehyde. In contrast, the s-*cis* enamine moiety of **1a** and **V** is primarily accessible from the *Si*-face due to the two aryl groups of the aminocatalyst. In reactions leading to cycloadducts **5**, the 2π-component is not shielded by a second catalyst unit and preferentially approaches the 12π-component from the *Si*-face.

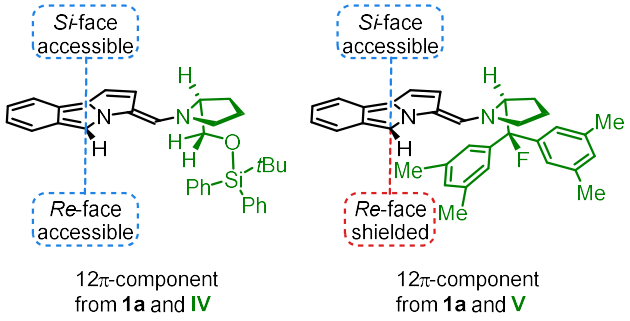

Figure 8: Facial shielding of 12π-components of **1a** and **IV** versus **1a** and **V**.

While the main advantage of the developed aminocatalytic strategy lies in the stereoselective formation of chiral benzo[*a*]cycl[3.2.2]azines, the observed oxidation of cycloadducts **5** prompted the investigation into directly forming their achiral, fully unsaturated counterparts. Through utilization of electron- deficient 2π-components carrying a nucleofugal substituent, the fully unsaturated benzo[*a*]cycl[3.2.2]azines **7a**–**c** (Figure 9) were formed through a cycloaddition-elimination sequence. Due to the tosyl moiety acting both as a leaving group and an electron-withdrawing group, the use of (*E*)-3-tosylacrylonitrile **6a** led to the formation of the chromatographically separable 4- and 5-substituted regioisomers **7a** and **7b** in a 4.5:1 ratio. Using the symmetrical (*E*)-1,2-bis(phenylsulfonyl)ethene **6b** gave only the 4-sulfonylated product **7c**, witnessing the preferential elimination of a leaving group in the 5-position. The three compounds **7a**–**c** possess photoluminescent properties with profiles similar to known benzo[*a*]cycl[3.2.2]azines.[7] Of these, **7a** displayed the highest fluorescence quantum yield (Φ_f = 0.23), thereby demonstrating that both the position and the nature of the electron-withdrawing group play an important role on the photoluminescence. Quantum yields, UV/Vis and fluorescence emission spectra for **7a**–**c** are included in the Supporting Information.

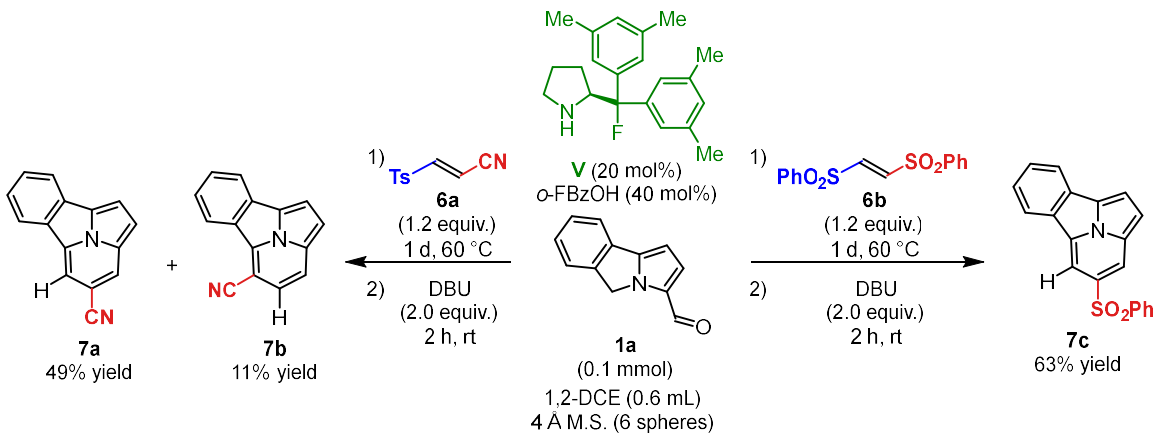

Figure 9: One-pot formation of fully unsaturated benzo[a]cycl[3.2.2]azines **7** from benzo[*a*]pyrrolizine-3-carbaldehyde **1a** and vinyl sulfones **6**.

Modifications of the benzo[a]cycl[3.2.2]azine core. Selective transformations of the [12+2] cycloadduct **5g** have been explored, revealing a high potential for its use as an electrophile with preservation of stereochemical information. Reduction with $NaBH_4$ generates **8** in good yield and high diastereoselectivity. Reacting **5g** with thiophenol delivered the crystalline adduct **9** in excellent yield. This compound contains four adjacent stereocenters, and the addition is highly diastereoselective toward the all-*trans*-adduct. The absolute configuration of **9** was determined through X-ray crystallographic analysis.

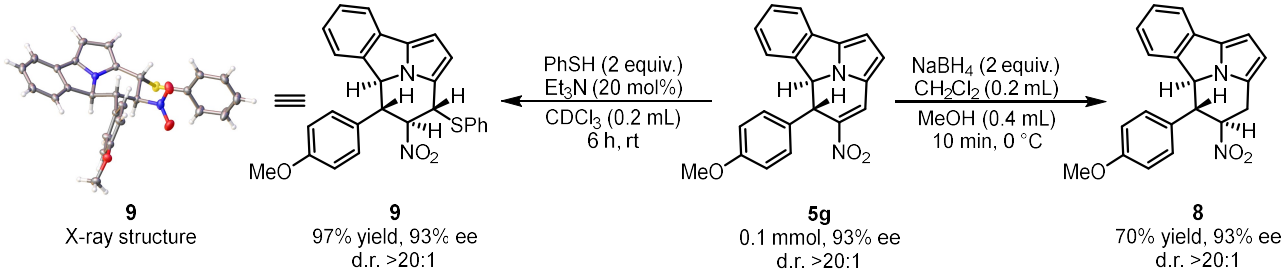

Isolated yields. Diastereomeric ratios determined by NMR analysis of isolated product. The enantiomeric excess values were determined by UPC[2].

Figure 10: Diastereoselective transformations of the [12+2] cycloadduct **5g** toward **8** and **9**, by reaction with $NaBH_4$ and thiophenol, respectively.

CONCLUSION

The hitherto arduous enantioselective construction of the cycl[3.2.2]azine core has been attained through a one-step procedure utilizing organocatalytic higher-order cycloaddition chemistry. A range of *in situ* generated electron-rich 12π-components based on 5*H*-benzo[*a*]pyrrolizine-3-carbaldehydes were brought to react with α,β-unsaturated aldehydes to form substituted *trans*-benzo[*a*]cycl[3.2.2]azines through a stepwise [12+2] cycloaddition in typically good yields with high and consistent stereoselectivities (35-84% yield, >7:1 d.r., 88-93% ee for 16 examples). While these cycloadducts are prone toward partial erosion of diastereomeric ratio during purification, one-pot reduction of the cycloadduct formyl group led to preservation of the stereochemical information. DFT calculations revealed that the energetic barrier for

ring-closure is crucial to the observed high stereoselectivity. Through minor modifications of reaction conditions, the scope was expanded to include *trans*-benzo[*a*]cycl[3.2.2]azines from α,β-unsaturated ketoesters (35-67% yield, 2.7:1-12.5:1 d.r., 84-93% ee for 4 examples) and nitroolefins (26-49% yield, >20:1 d.r., 93% ee for 3 examples) which, likely due to a change in catalyst stoichiometry, were formed with inversion in enantioselectivity compared to the products derived from α,β-unsaturated aldehydes. It was demonstrated that the [12+2] cycloadducts undergo highly diastereoselective transformations, witnessing a high potential for their use as Michael acceptors. In addition, fully unsaturated and photoluminescent benzo[*a*]cycl[3.2.2]azines were obtained using vinyl sulfones, which demonstrated that both the position and the nature of the electron-withdrawing group play an important role on the quantum yield.

SUPPORTING INFORMATION

Supplementary optimization tables, experimental procedures, characterization of substrates and products, X-ray crystallographic data, ground state and transition state structures of intermediates for the formation of cycloadduct **3b**, experimental and calculated data for the ECD spectra of **3h'** and **5g**, UV/Vis as well as fluorescence emission spectra and quantum yields for **7a**–**c**.

AUTHOR INFORMATION.

*Karl Anker Jørgensen: kaj@chem.au.dk

NOTES

The authors declare no competing financial interest.

ACKNOWLEDGEMENTS.

KAJ thanks Villum Investigator grant (no. 25867), the Carlsberg Foundation "Semper Ardens" and Aarhus University. We thank Dr. Joseph A. Izzo for discussions and mentorship in DFT calculations. We also thank Mathias Kirk Thøgersen for elucidation of X-ray structures, Professor Jesper Bendix, University of Copenhagen, for his assistance with obtaining ECD spectra and Dr. Thomas Breitenbach for assisting with emission spectra and determination of quantum yields. The numerical, computational results presented in this work were obtained at the Centre for Scientific Computing, Aarhus University http://phys.au.dk/forskning/cscaa/.

REFERENCES

[1] a) McLeod, D.; Thøgersen, M. K.; Jessen, N. I.; Jørgensen, K. A.; Jamieson, C. S.; Xue, X.-S.; Houk, K. N.; Liu, F.; Hoffmann, R. Expanding the Frontiers of Higher-Order Cycloadditions. *Acc. Chem. Res.* **2019**, *52*, 3488–3501. b) Mose, R.; Preegel, G.; Larsen, J.; Jakobsen, S.; Iversen, E. H.; Jørgensen, K. A. Organocatalytic Stereoselective [8+2] and [6+4] Cycloadditions. *Nat. Chem.* **2017**, *9*, 487–492. c) Zhou,

Z.; Wang, Z.-X.; Zhou, Y.-C.; Xiao, W.; Ouyang, Q.; Du, W.; Chen, Y. C. Switchable Regioselectivity in Amine-catalysed Asymmetric Cycloadditions. *Nat. Chem.* **2017**, *9*, 590–594. d) Bertuzzi, G.; Thøgersen, M. K.; Giardinetti, M.; Vidal-Albalat, A.; Simon, A.; Houk, K. N.; Jørgensen, K. A. Catalytic Enantioselective Hetero-[6+4] and -[6+2] Cycloadditions for the Construction of Condensed Polycyclic Pyrroles, Imidazoles, and Pyrazoles. *J. Am. Chem. Soc.* **2019**, *141*, 3288–3297. c) Frankowski, S.; Skrzyńska, A.; Albrecht, Ł. Inverting the Reactivity of Troponoid Systems in Enantioselective Higher-order Cycloaddition. *Chem. Commun.* **2019**, *55*, 11675–11678. Chen, X.; Thøgersen, M. K.; Yang, L.; Lauridsen, R. F.; Xue, X.-S.; Jørgensen, K. A.; Houk, K. N. [8+2] vs [4+2] Cycloadditions of Cyclohexadienamines to Tropone and Heptafulvenes—Mechanisms and Selectivities. *J. Am. Chem. Soc.* **2021**, DOI: 10.1021/jacs.0c10966.

[2] For examples of indolizidine- and quinolizidine alkaloids, see: Michael, J. P. *Nat. Prod. Rep.* **2008**, *25*, 139–165.

[3] a) Boekelheide, V.; Windgassen, R. J. Cyclazines. The Synthesis of a New Class of Aromatic Compounds. *J. Am. Chem. Soc.* **1958**, *80*, 2020. b) Windgassen Jr., R. J.; Saunders Jr., W. H.; Boekelheide, V. Cyclazines. A New Class of Aromatic Heterocycles. *J. Am. Chem. Soc.* **1959**, *81*, 1459–1465.

[4] Wu, Z.-l.; Wang, Q.; Wang, J.-x.; Dong, H.-y.; Xu, X.-k.; Shen, Y.-h.; Li, H.-l.; Zhang, W.-d. Vlasoulamine A, a Neuroprotective [3.2.2]Cyclazine Sesquiterpene Lactone Dimer from the Roots of Vladimiria Souliei. *Org. Lett.* **2018**, *20*, 7567–7570.

[5] Ondrus, A. E.; Movassaghi, M. Total Synthesis and Study of Myrmicarin Alkaloids. *Chem. Commun.* **2009**, 4151–4165.

[6] a) Jørgensen, A. S.; Jacobsen, P.; Christiansen, L. B.; Bury, P. S.; Kanstrup, A.; Thorpe, S. M.; Bain, S.; Nærum, L.; Wassermann, K. Synthesis and Pharmacology of a Novel Pyrrolo[2,1,5-*cd*]indolizine (NNC 45-0095), a High Affinity Non-Steroidal Agonist for the Estrogen Receptor. *Bioorg. Med. Chem. Lett.* **2000**, *10*, 399–402. b) Jørgensen, A. S.; Jacobsen, P.; Christiansen, L. B.; Bury, P. S.; Kanstrup, A.; Thorpe, S. M.; Nærum, L.; Wassermann, K. Synthesis and Estrogen Receptor Binding Affinities of Novel Pyrrolo[2,1,5-*cd*]indolizine Derivatives. *Bioorg. Med. Chem. Lett.* **2000**, *10*, 2383–2386.

[7] a) Mitsumori, T.; Bendikov, M.; Dautel, O.; Wudl, F.; Shioya, T.; Sato, H.; Sato, Y. Synthesis and Properties of Highly Fluorescent Indolizino[3,4,5-*ab*]isoindoles. *J. Am. Chem. Soc.* **2004**, *126*, 16793–16803. b) Yang, D.-T.; Radtke, J.; Mellerup, S. K.; Yuan, K.; Wang, X.; Wagner, M.; Wang, S. One-Pot Synthesis of Brightly Fluorescent Mes_2B-Functionalized Indolizine Derivatives via Cycloaddition Reactions. *Org. Lett.* **2015**, *17*, 2486–2489.

[8] Batroff, V.; Flitsch, W.; Leaver, D.; Skinner, D. An improved Synthesis of Cyclazines from 3*H*-Pyrrolizines. *Chem. Ber.* **1984**, *117*, 1649–1658.

[9] a) Belei, D.; Abuhaie, C.; Bicu, E.; Jones, P. G.; Hopf, H.; Birsa, L. M. A Direct Synthesis of Octahydropyrrolo[2,1,5-*cd*]indolizin-6-one Derivatives. *Synlett* **2012**, *23*, 545–548. b) Liu, R.; Wang, X.; Sun, J.; Yan, C.-G. A Facile Synthesis of Tricyclic Skeleton of Alkaloid 261C by Double [3+2] Cycloaddition of Pyridinium Ylide. *Tetrahedron Lett*. **2015**, *56*, 6711–6714.

[10] Galbraith, A.; Small, T.; Barnes, R. A.; Boekelheide, V. The Formation of Cycl[3.2.2]azine Derivatives via the Reaction of Pyrrocoline with Dimethyl Acetylenedicarboxylate. *J. Am. Chem. Soc.* **1961**, *83*, 453–458.

[11] a) Kuznetsov, A. G.; Bush, A. A.; Babaev, E. V. Synthesis and Reactivity of 5-Br(I)-indolizines and their Parallel Cross-coupling Reactions. *Tetrahedron* **2008**, *64*, 749–756. b) Uchida, T.; Matsumoto, K. Cycloaddition Reaction of 3-Cyanoindolizines with Dimethyl Acetylenedicarboxylate—[3.2.2]azines and 1:2 Adducts. *Chem. Lett.* **1980**, *9*, 149–150.

[12] Kajigaeshi, S.; Mori, S.; Fujisaki, S.; Kanemasa, S. Exo-selective Peripheral Cycloaddition Reactions of Pyrido[2,1-*a*]isoindole. *Bull. Chem. Soc. Jpn.* **1985**, *58*, 3547–3551.

[13] a) Johnson, D.; Jones, D. Reaction between 3*H*-Pyrrolizines and Acetylenedicarboxylic Esters. Part I. Preparation of 3-(AIkoxycarbonylmethylene)-3*H*-pyrrolizines. *J. Chem. Soc., Perkin Trans. 1* **1972**, 840–844. b) Jessep, M. A.; Leaver, D. Heterocyclic Compounds with Bridgehead Nitrogen Atoms. Part 7. The Synthesis of Pyrrolo[2,1,5-*cd*]indolizines ([2,2,3]Cyclazines) and Pyrazino[2,1,6-*cd*]pyrrolizines (6-Aza[2,2,3]cyclazines) from 3*H*-Pyrrolizine. *J. Chem. Soc., Perkin Trans. 1* **1980**, 1319–1323.

[14] a) Sayah, B.; Pelloux-Léon, N.; Vallée, Y. First Synthesis of Nonracemic (R)-(+)-Myrmicarin 217. *J. Org. Chem.* **2000**, *65*, 2824–2826. b) Settambolo, R.; Guazzelli, G.; Lazzaroni, R. Intramolecular Cyclodehydration of (4S)-(+)-4-Carboxyethyl-4-(pyrrol-1-yl)butanal as the Key Step in the Formal Synthesis of (S)-(−)-Myrmicarin 217. *Tetrahedron: Asymmetry* **2003**, *14*, 1447–1449. c) Movassaghi, M.; Ondrus, A. E. Enantioselective Total Synthesis of Tricyclic Myrmicarin Alkaloids. *Org. Lett.* **2005**, *7*, 4423–4426. d) Angle, S. R.; Qian, X. L.; Pletnev, A. A.; Chinn, J. General Synthesis of Pyrroloquinolizidines: Synthesis of an Unnatural Homologue of the Pyrroloindolizidine Myrmicarin Alkaloid 215B. *J. Org. Chem.* **2007**, *72*, 2015–2020. e) Santarem, M.; Vanucci-Bacqué, C.; Lhommet, G. Formal Total Synthesis of Enantiopure Tricyclic (S)-Myrmicarin Alkaloids 217, 215A and 215B. *Heterocycles* **2010**, *81*, 2523–2537.

[15] a) Donslund, B. S.; Jessen, N. I.; Bertuzzi, G.; Giardinetti, M.; Palazzo, T. A.; Christensen, M. L.; Jørgensen, K. A. Catalytic Enantioselective [10+4] Cycloadditions. *Angew. Chem. Int. Ed.* **2018**, *57*, 13182–13186. b) Giardinetti, M.; Jessen, N. I.; Christensen, M. L.; Jørgensen, K. A. Organocatalytic [10+4] Cycloadditions for the Synthesis of Functionalised Benzo[*a*]azulenes. *Chem. Commun.* **2019**, *55*, 202–205.

[16] Mayer, A.; Meier, H. 1*H*-Naphtho[2,1-*b*]thiete and 2*H*-Naphtho[2,3-*b*]thiete—Synthesis and Reactivity. *Tetrahedron Lett.* **1994**, *35*, 2161–2164.

[17] Reviews touching on the subject of vinylogous enamine catalysis include: a) Jia, Z.-J.; Jiang, H.; Li, J.-L.; Gschwend, B.; Li, Q.-Z.; Yin, X.; Grouleff, J.; Chen, Y.-C.; Jørgensen, K. A. Trienamines in Asymmetric Organocatalysis: Diels−Alder and Tandem Reactions. *J. Am. Chem. Soc.* **2011**, *133*, 5053–5061; b) Marcos, V.; Alemán, V. Old Tricks, New Dogs: Organocatalytic Dienamine Activation of α,β-Unsaturated Aldehydes. *Chem. Soc. Rev.* **2016**, *45*, 6812–6832; c) Curti, C.; Battistini, L.; Sartori, A.; Zanardi, F. New Developments of the Principle of Vinylogy as Applied to π-Extended Enolate-Type Donor Systems. *Chem. Rev.* **2020**, *120*, 2448–2612.

[18] Gerasyuto, A. I.; Hsung, R. P.; Sydorenko, N.; Slafer, B. A Formal [3+3] Cycloaddition Reaction. 5. An Enantioselective Intramolecular Formal Aza-[3+3] Cycloaddition Reaction Promoted by Chiral Amine Salts. *J. Org. Chem.* **2005**, *70*, 4248–4256.

[19] For the synthesis of **1a**, see: Laha, J. K.; Bhimpuria, R. A.; Hunjan, M. K. Intramolecular Oxidative Arylations in 7-Azaindoles and Pyrroles: Revamping the Synthesis of Fused *N*-Heterocycle Tethered Fluorenes. *Chem. Eur. J.* **2017**, *23*, 2044–2050.

[20] a) Puchot, C.; Samuel, O.; Duñach, E.; Zhao, S.; Agami, C.; Kagan, H. B. Nonlinear Effects in Asymmetric Synthesis. Examples in Asymmetric Oxidations and Aldolization Reactions. *J. Am. Chem. Soc.* **1986**, *108*, 2353–2357. b) Guillaneux, D.; Zhao, S.-H.; Samuel, O.; Rainford, D.; Kagan, H. B. Nonlinear Effects in Asymmetric Catalysis. *J. Am. Chem. Soc.* **1994**, *116*, 9430−9439. c) Girard, C.; Kagan, H. B. Nonlinear Effects in Asymmetric Synthesis and Stereoselective Reactions: Ten Years of Investigation. *Angew. Chem. Int. Ed.* **1998**, *37*, 2922−2959. d) Satyanarayana, T.; Abraham, S.; Kagan, H. B. Nonlinear Effects in Asymmetric Catalysis. *Angew. Chem. Int. Ed.* **2009**, *48*, 456−494.

[21] Frisch, M. J.; Trucks, G. W.; Schlegel, H. B.; Scuseria, G. E.; Robb, M. A.; Cheeseman, J. R.; Scalmani, G.; Barone, V.; Mennucci, B.; Petersson, G. A.; Nakatsuji, H.; Caricato, M.; Li, X.; Hratchian, H. P.; Izmaylov, A. F.; Bloino, J.; Zheng, G.; Sonnenberg, J. L.; Hada, M.; Ehara, M.; Toyota, K.; Fukuda, R.; Hasegawa, J.; Ishida, M.; Nakajima, T.; Honda, Y.; Kitao, O.; Nakai, H.; Vreven, T.; Montgomery, J. A.; Peralta, J. E.; Ogliaro, F.; Bearpark, M.; Heyd, J. J.; Brothers, E.; Kudin, K. N.; Staroverov, V. N.; Kobayashi, R.; Normand, J.; Raghavachari, K.; Rendell, A.; Burant, J. C.; Iyengar, S. S.; Tomasi, J.; Cossi, M.; Rega, N.; Millam, J. M.; Klene, M.; Knox, J. E.; Cross, J. B.; Bakken, V.; Adamo, C.; Jaramillo, J.; Gomperts, R.; Stratmann, R. E.; Yazyev, O.; Austin, A. J.; Cammi, R.; Pomelli, C.; Ochterski, J. W.; Martin, R. L.; Morokuma, K.; Zakrzewski, V. G.; Voth, G. A.; Salvador, P.; Dannenberg, J. J.; Dapprich, S.; Daniels, A. D.; Farkas, Ö.; Foresman, J. B.; Ortiz, J. V.; Cioslowski, J.; Fox, D. J. *Gaussian 09*, revision D.01; Gaussian, Inc.: Wallingford, CT, 2009.

[22] a) Becke, A. D. Density-Functional Thermochemistry. III. The Role of Exact Exchange. *J. Chem. Phys.* **1993**, *98*, 5648–5652. b) Lee, C.; Yang, W.; Parr, R. G. Development of the Colle-Salvetti Correlation-energy Formula into a Functional of the Electron Density. *Phys. Rev. B* **1988**, *37*, 785−789. c) Stephens, P. J.; Devlin, F. J.; Chabalowski, C. F.; Frisch, M. J. *Ab Initio* Calculation of Vibrational Absorption and

Circular Dichroism Spectra Using Density Functional Force Fields. *J. Phys. Chem.* **1994**, *98*, 11623−11627. d) Hariharan, P. C.; Pople, J. A. The Influence of Polarization Functions on Molecular Orbital Hydrogenation Energies. *Theoret. Chim. Acta* **1973**, *28*, 213−222.
[23] a) Grimme, S.: Ehrlich, S.: Goerigk, L. Effect of the Damping Function in Dispersion Corrected Density Functional Theory. *J. Comput. Chem.* **2011**, *32*, 1456−1465. b) Weigend, F.; Ahlrichs, R. Balanced Basis Sets of Split Valence, Triple Zeta Valence and Quadruple Zeta Valence Quality for H to Rn: Design and Assessment of Accuracy. *Phys. Chem. Chem. Phys.* **2005**, *7*, 3297–3305. c) Marenich, A. V.; Cramer, C. J.; Truhlar, D. G. Universal Solvation Model Based on Solute Electron Density and on a Continuum Model of the Solvent Defined by the Bulk Dielectric Constant and Atomic Surface Tensions. *J. Phys. Chem. B* **2009**, *113*, 6378−6396.

Graphical Abstract